Integration between calibrated time-of-flight camera data and multi-image matching approach for architectural survey

Integration between calibrated Time-of-Flight camera data and multi-image matching approach for architectural survey

F. Chiabrando[a], F. Nex[b], D. Piatti*[b], F. Rinaudo[b]
[a]Dept. of Human Settlements Science and Technology, Politecnico di Torino, Viale Mattioli 39, 10125 Torino, Italy;
[b]Dept. of Dept. of Land, Environment and Geo-Engineering , Politecnico di Torino, C.so Duca degli Abruzzi 24, 10121 Torino, Italy

ABSTRACT

In this work, the integration between data provided by Time-of-Flight cameras and a multi-image matching technique for metric surveys of architectural elements is presented. The main advantage is given by the quickness in the data acquisition (few minutes) and the reduced cost of the instruments. The goal of this approach is the automatic extraction of the object breaklines in a 3D environment using a photogrammetric process, which is helpful for the final user exigencies for the reduction of the time needed for the drawing production. The results of the performed tests on some architectural elements will be reported in this paper.

Keywords: Time-of-Flight, calibration, multi-image matching, automatic drawing, breakline extraction, edge extraction, 3D modelling

1. INTRODUCTION

The production of architectural surveys usually requires complete and reliable geometrical information about the object to be described. Traditionally, this information is obtained using time-consuming surveys (total stations, levels, etc.) or performing manual photogrammetric plottings. In the last few years, the introduction of LiDAR instruments has allowed to quickly acquire complete point clouds of the object to be surveyed. Nevertheless, this data cannot be directly used to produce 2D representations (plans and sections) because of the difficulty to extract geometric primitives (e. g. lines, surfaces, volumes, …) from a 3D point cloud. Moreover, several manual interventions have to be usually performed on the extracted data since no automatic and reliable procedures have been achieved up to now.

In order to represent metrically correct object geometries it is necessary to measure and extract, from the survey data, the breaklines that allow the artifact to be described at the requested representation scale.

The total station survey is often employed for accurately measure the breaklines and the GCPs (Ground Control Points) useful to define a local reference system for the photogrammetric process and for the LiDAR survey. Nevertheless, a complete survey of an artifact with complex geometry only using topographic instruments could be time consuming; for this reason, in many cases, this technique is integrated with photogrammetric surveys and/or LiDAR surveys.

The photogrammetric approach is advantageous for the data acquisition time, but the data processing and plotting are usually time consuming due to the necessity of several manual interventions. The LiDAR technique allows a huge number of points to be quickly acquired with a precision that mainly depends on the employed instrument; however, the main drawbacks are the high cost of the instruments and the long time needed for the data processing. Hence, each survey technique has pros and cons and each of them allows an object to be surveyed with a different accuracy; therefore, in order to achieve a more accurate and complete survey, it is usually necessary to integrate the information coming from more than one of the aforementioned techniques.

The main objective of this work is to propose a low cost approach that follows two different aims: quickness in the data acquisition and automatic breakline extraction in order to ease and speed up the drawing production of architectural elements. The approach is based on the employment of a Time-of-Flight (ToF) camera (also called 3D camera) for the generation of an approximate Digital Surface Model (DSM) to be used in a multi-image matching approach that allows the object breaklines to be automatically extracted. Previous works[1, 2] have already shown good results considering the

*dario.piatti@polito.it; phone +39 011 090 7657; fax +39 011 090 7699; http://polito.academia.edu/dariopiatti

integration between LiDAR data and multi-image matching techniques, while in this paper the extension to the ToF data is presented. In the following sections the acquisition phases, the data processing steps and the first results obtained by the Geomatics research group of the Politecnico di Torino are reported.

2. TOF CAMERAS

ToF cameras are an emerging technology which allows to acquire 3D point clouds, which are almost comparable with those of traditional LiDAR instruments, at video frame rates. Using these cameras, a bundle of distances is determined simultaneously for each pixel of a two-dimensional sensor array. The measured distances are obtained from the time an emitted signal takes to return to the camera. Two main variations of the ToF principle have been implemented above all: one measures distance by means of direct measurement of the runtime of a travelled light pulse using arrays of single-photon avalanche diodes (SPADs)[3]. The other method uses amplitude modulated light and obtains distance information by measuring the phase difference between a reference signal and the reflected signal[4]. While complex readout schemes and low frame rates have prevented the use of SPAD arrays in commercial 3D-imaging products up to now, the second category has already been implemented successfully in several commercially available 3D camera systems, such as the two ToF cameras reported in Table 1.

Table 1. SwissRanger-4000 (SR-4000) and PMD CamCube 3.0 technical specifications.

TECNICAL SPECIFICATIONS	**SR-4000**	**PMD CamCube 3.0**
	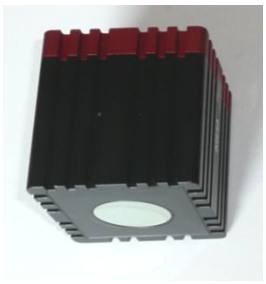	
Focal length [mm]	10	12.8
Pixel array size [-]	176 (h) x 144 (v)	200 x 200
Pixel pitch [mm]	40	not available
Fileld of view [°]	43.6 (h) x 34.6 (v)	40 (h) x 40 (v)
Working range with standard settings [m]	0.3-5.0	0.3-7.0
Repeatability (1σ) [mm]	4 (typical) - 7 (maximum) (@ 2 m working range and 100% target reflectivity)	< 3 (@ 4 m working range and 75% target reflectivity)
Absolute accuracy [mm]	±10 (@ 100% target reflectivity	not available
Frame rate [fps]	up to 54 (depending on camera settings)	up to 40 (depending on camera settings)

Although ToF cameras are usually characterized by no more than a few thousands of tens of pixels, a maximum unambiguous measurement range up to thirty meters can be reached and complete 3D point clouds of the analyzed objects can be quickly acquired. These devices allow generating point clouds such as in the case of the LiDAR technique and photogrammetry but with the great advantage of real time acquisition, low cost and handiness. Unlike photogrammetric techniques, 3D cameras allow a point cloud to be obtained of the object that has to be surveyed from even only one point of view, without the need of any particular lighting conditions, since these cameras are active sensors that work outside of the visible spectrum. However, ToF cameras have similar drawbacks to LiDAR techniques

about the impossibility to directly obtain radiometric and semantic information and to describe the exact position of the object breaklines.

ToF cameras usually deliver a range image and an amplitude image with infrared modulation intensities at video frame rates. The range image (or depth image) contains for each pixel the radial measured distance between the considered pixel and its projection on the observed object, while the amplitude image contains for each pixel the strength of the reflected signal by the object. In some cases an intensity image is also delivered, which represents the mean of the total light incident on the sensor (reflected modulated signal and background light of the observed scene).

Nevertheless, ToF camera measurements usually suffer from some systematic errors that have to be corrected by using suitable calibration procedures in order to refine the measurement accuracy[5-10]. Moreover, systematic errors can occur which are scene dependent as they vary according to the surveyed area, such as: the "multipath" effect[11], the "scattering artifact"[12] and the so called "mixed pixels"[13]. All these error sources worsen the achievable measurement accuracy, which is usually limited to about one centimeter in the best case.

In this work, the Swiss-Ranger-4000 (SR-4000) camera was employed. This camera is characterized by a 176 x 144 pixel array and a working range from 0.3 m to 5 m (Table 1). For more details about camera specifications see [11].

All the acquired data were corrected with the distance error model proposed in [14], which refines the camera distance measurement accuracy up to 1 cm. Some tests about the influence of object reflectivity on the SR-4000 measurements on common materials are reported in [15]. In that paper, it was outlined that the distance measurement accuracy variations caused by the different reflectivity of the tested objects are of the same order of the camera absolute accuracy reported in [11]; however, it is worth nothing that some materials can generate a high number of saturated pixels and, therefore, determine many wrong measurements. Moreover, in [14] it has been shown that a camera warm-up of about 40 minutes should be performed in order to achieve a good stability of the camera distance measurements.

In order to test the potentiality of ToF cameras for architectural surveys and for their integration with other techniques, some tests on two windows of the Castello del Valentino (the headquarter of the Architecture Faculty of the Politecnico di Torino), have been performed. In particular, the 3D point clouds acquired with the ToF camera were processed and used as approximate DSM for the multi-matching approach described in section 3.

3. MULTI-IMAGE MATCHING APPROACH

The automated extraction of objects from photogrammetric images has been a topic of research for decades. Nowadays, image-matching techniques allow a great number of points to be extracted in a quick way. In particular, the multi-image matching techniques allow an improvement in the geometric precision and the reliability with respect to image pairs, by extracting points and edges from images and projecting their match in the space[16]. Actually, this kind of solution requires an approximate DSM in order to "drive" the solution to the correct match; the more accurate is this model, the more correct (without blunders) is the solution.

Image matching techniques have shown good results in aerial applications. In particular, multi-image techniques have improved the results in terms of precision and reliability[16], and allowed a point cloud density comparable to the LiDAR one to be obtained. These techniques consider the epipolar geometry between images in order to reduce the search area in adjacent images, and thus decreasing the number of blunders to a great extent. The run on the epipolar line is further reduced by the z-value, which is provided by an approximate DSM. Nevertheless, the z value varies smoothly in aerial cases, compared to the relative flight height. The height differences between the top and the bottom of the buildings are small, compared to the taking distance. In these conditions, the approximate DSM can be achieved by using interest operators in the feature extraction and matching.

In contrast, the terrestrial case shows greater z-value differences: façades are usually rough with balconies, columns or decorations that protrude of several meters. In these conditions, z-values provided by approximate DSM are not sufficient to limit the run of the epipolar line especially in presence of significant depth variations[1, 17]: blunders are more frequent during the matching procedure and it is still difficult to filter them. These variations are more relevant as they can be 1/5 of the taking distance. In this situation, z-values provided by approximate DSM (created through a photogrammetric approach) are not sufficient to limit the run of the epipolar line: blunders are more frequent during the matching procedure and it is still difficult to filter them. Furthermore, the façade texture is often not good enough to

allow effective matching techniques to be performed: blank areas in automatically extracted point cloud are very common in correspondence of painted walls. Until now, fully matching techniques have only achieved good results in bas-relief or in limited area surveys. In order to overcome these problems, the photogrammetric process can be helped by the ToF camera data. The main idea is to use the reliable information provided by this instrument as DSM in the matching algorithms.

3.1 Breakline extraction algorithm

The proposed algorithm can be summarized into several steps, which are shown in Figure 1 left. In particular, the steps where the ToF data gives additional information to the multi-image matching approach are highlighted in orange colour.

The images are acquired according to an *ad hoc* taking configuration (Figure 1 right): several images are acquired and the most central one is considered as reference image during the matching process. The ToF point cloud is acquired from a central position with respect to the image acquisition in order to have approximately the same occluded areas in the ToF data and in the reference image.

All images are previously restored and then enhanced. The image restoration is performed by means of an Adaptive Gaussian smoothing[2] that filters the image according to the noise level evaluated on the uniform areas of the image. Then, the image enhancement is achieved using a Wallis filter[18]. In general, the image pre-processing allows the number of detected edges to be increased with respect to the original image.

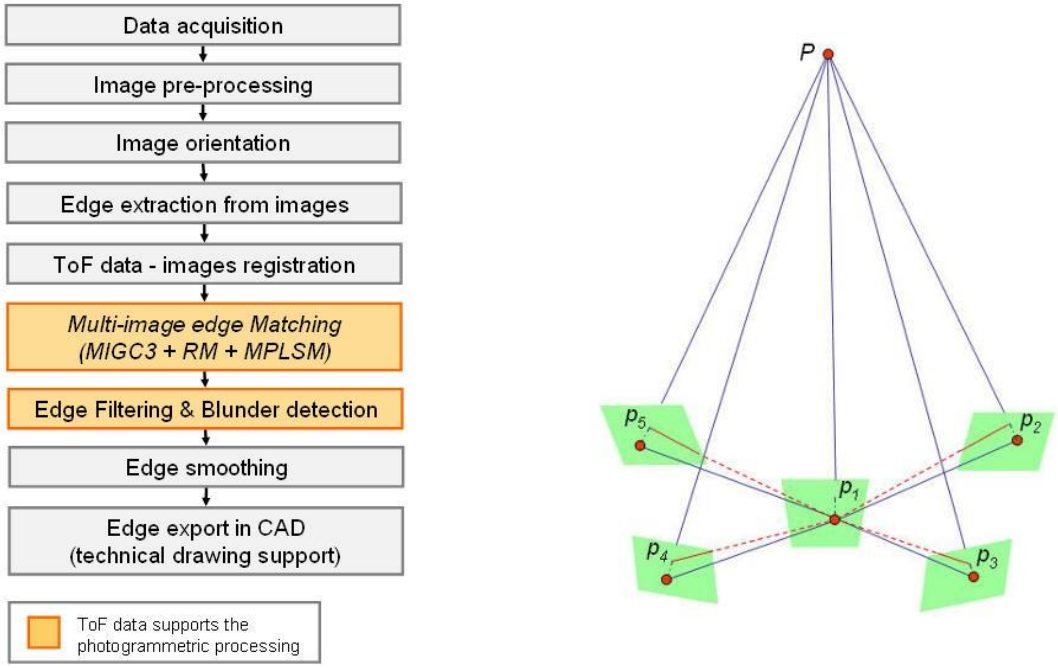

Figure 1. Breakline extraction workflow (left) and ad hoc image taking configuration (right).

The orientation is performed in a proper reference system in order to have the z-coordinate normal to the main plain of the façade. In this step, the A[2]SIFT (Auto-Adaptive Scale Invariant Feature Transform) operator[19] is adopted in the tie-point extraction and a robust (Least Median Square) relative orientation is then performed in order to eliminate the mismatches[20]. Finally, a bundle block adjustment is performed. After that, the edge extraction is performed by the Canny operator[21] on the reference image. The extracted edges are then approximated, by identifying the pixels where the edge changes in direction as knots and linking these dominant points by straight edges.

The point cloud is registered in the photogrammetric reference system by means of a spatial similarity transformation. In this way, it is possible to share the information between the images and the point cloud. Then, a multi-image matching algorithm is set up. The algorithm is a modification of the Geometrically Constrained Cross Correlation (GC[3])[16]: it uses a

multi-image approach, that is, it considers a reference image and projects the image patch (of each dominant point) of the reference image onto the DSM (ToF point cloud), and then, using the approximate z-value achieved by the DSM, back-projects it onto the other images. Through this algorithm, the dominants points of each edge are matched in all the images in order to reconstruct the breakline positions in 3D. The images are preliminarily undistorted (using the camera calibration) in order to ease them into a central perspective. The epipolar constraint limits the search space in the images. The length of this line could be achieved considering the z-value given by the ToF point cloud; then, in order to find the homologous point in all the images, this value is varied into a range (Δz). This work is enforced and improved through the position of already matched points: the z-value of two adjacent dominant points on the same edge must be similar. In this way, it is possible to reduce the run of the epipolar line on the façade to few centimetres. In order to improve the rate of the successfully matched points, a relational matching has been developed. This algorithm integrates the figural continuity constraint through a probability relaxation approach[22] and it is able to solve several ambiguities of the matching process. The method uses the already matched dominants points as anchors and in an iterative way defines the more suitable match between candidates imposing a smoothing constraint. Finally, a Multi-Image Least Square Matching (MILSM)[23] has been performed for each extracted point, in order to improve the accuracy up to a sub-pixel dimension.

During the matching process, some blunders can be generated. These blunders are firstly deleted from the extracted edges using a filter which considers the reciprocal point positions on the same edge: in particular, the position of a point is predicted considering the neighbouring points of the edge and, then, the difference between the predicted and the real position of the point is evaluated. If the difference value is higher than a predefined threshold, the point is deleted. This filter is not robust: it will work well if the blunders are isolated from each other. For this reason, a second filter could be used to clean the edges when several blunders are close together; this algorithm uses the ToF information to verify the correctness of each dominant point: when it is farther than a defined threshold from the point cloud, it is deleted.

Then, the image matching allows radiometric edges to be extracted. Most of these edges are due to shadows or radiometric changes but they have no a geometric correspondence. Only geometric boundaries are of interest in the surveying graphic drawings and for modelling purposes. For this reason, the position of each dominant point on the extracted edges is considered with respect to the ToF point cloud: it is verified whether a geometric discontinuity occurs in the ToF data close to the edge point.

The edges extracted by the matching algorithm are random noise affected and they cannot be directly used in the drawing production. For this reason, the noisy edges are split in basic elements (linear and curved elements) and each element is smoothed and eased, in an automatic way, into lines and second order curves by means of a polynomial fitting. Then, the basic elements are recollected in a unique smoothed edge[2].

Finally, geometric edges are exported in CAD in order to give preliminary data for the graphic drawing realization of the survey and for a rough evaluation of the achieved results.

4. DATA INTEGRATION

The proposed approach was tested on two windows of the Castello del Valentino. The first window (Figure 2 left) is plastered, while the second one (Figure 2 right) is made of brick. In both cases, the texture is not good enough for the traditional image matching approach to be performed. In the following sections, the data acquisition and processing information are reported for both the ToF camera and the multi-image matching approach.

4.1 ToF data acquisition

After the camera warm-up, the SR-4000 camera was positioned on a photographic tripod and moved to different positions in order to achieve a complete coverage of both the windows to be surveyed (Figure 2). Thirty frames were acquired from each position using the software delivered with the camera (SR_3D_View software), adjusting the integration time in order to have the minimum possible number of saturated pixels but a low noise level of the distance measurements.

In order to obtain a complete 3D model of each window, the ToF data was acquired from several different positions, with a good overlap between the acquired range images. As shown in Figure 3 right, some problems occurred during ToF data acquisition in the second case: the presence of the window glasses and of some parts of the window directly hit by the sun caused quite noisy measurements and some pixels to be often saturated.

Figure 2. The two windows of the Castello del Valentino to be surveyed and ToF data acquisition.

4.2 ToF data processing

The thirty frames acquired from each position were averaged in order to reduce the measurement noise. Then, the distance of each pixel of the averaged frames was corrected with the distance error model proposed in [14]. The medium distance between each point was about 0.015 m.

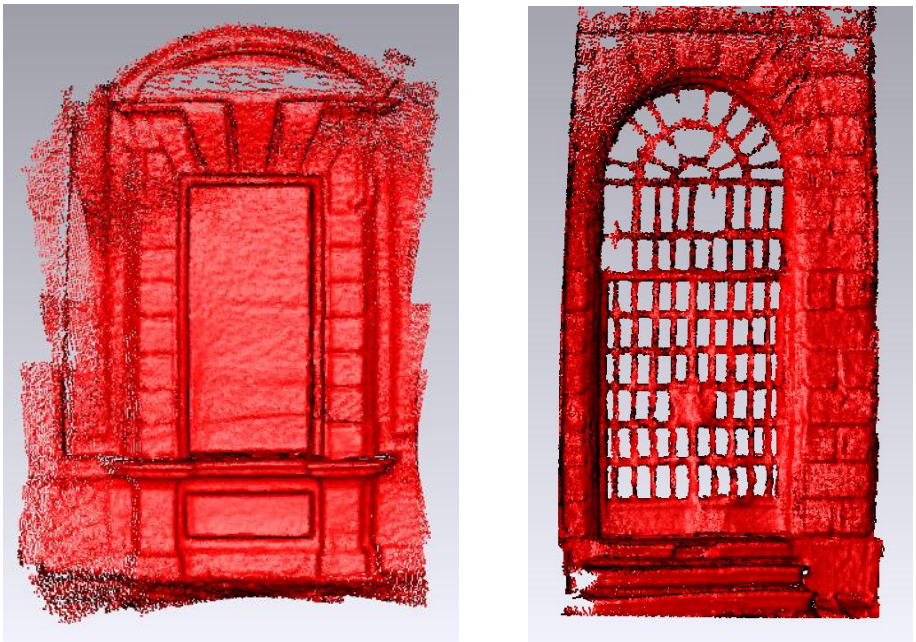

Figure 3. Screen-shots of the complete 3D ToF point cloud for both the surveyed windows.

Then, the obtained point clouds were registered using the ICP algorithm implemented in the Geomagic Studio® software in order to obtain a unique 3D model for each window (Figure 3). From this products, two dense DSMs were generated and then employed for the multi-image matching approach in order to extract the breaklines needed for the 2D representation of the two windows.

4.3 Image acquisition

The image acquisition was performed using the *Canon Eos-5D Mark II* digital camera equipped with a 24 mm lens. The taking distance was about 5-6 m. Five images were acquired for both windows according to the *ad hoc* configuration reported in Figure 1 right. According to this particular configuration the epipolar lines run in tilted direction with respect to the main lines of the façade (horizontal and vertical), and the homologous points can be determined in an

unambiguous way. Thanks to the image dimension (5616 x 3744 pixels) and the short taking distance, an excellent image resolution was reached (less than 2 mm of Ground Sample Distance (GSD)).

4.4 Data processing and results

The integration between ToF data and digital images has been performed according to the workflow reported in Figure 1 left. The edge extraction allowed a complete set of lines to be defined from the reference image of each case: Figure 4a and Figure 5a show the extracted edges, which are described by 45636 dominant points for the first window and 181596 for the second one.

a) b) c)

Figure 4. Extracted edges on the reference image a) and smoothed edges b) e c).

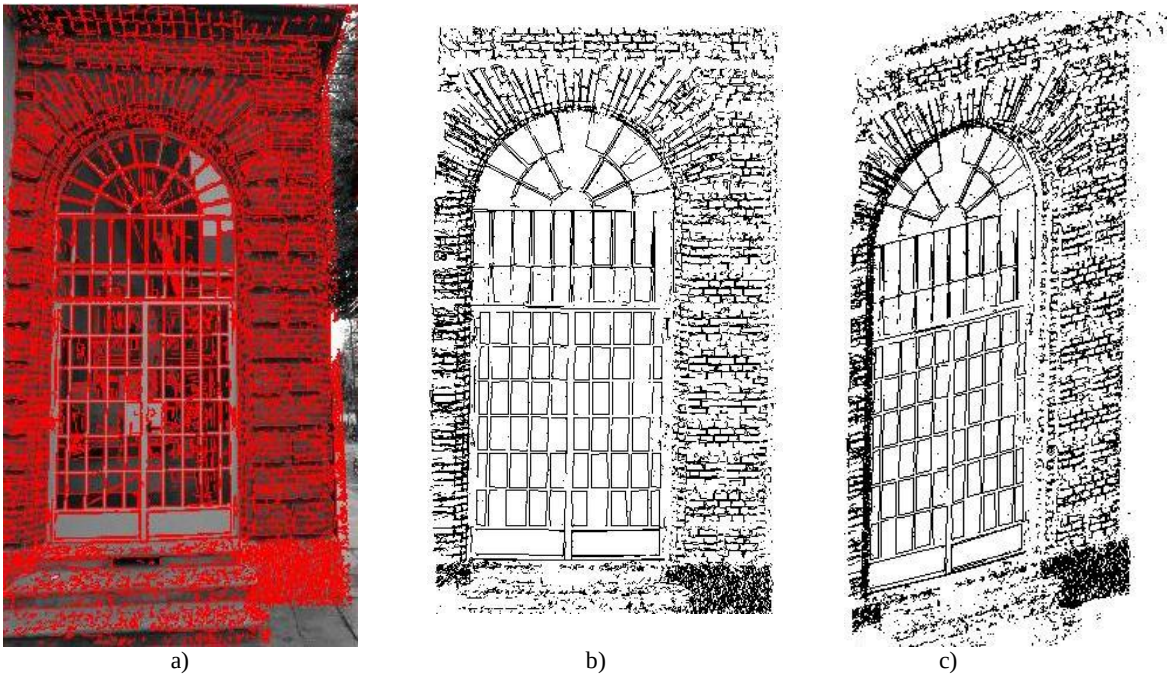

a) b) c)

Figure 5. Extracted edges on the reference image a) and smoothed edges b) e c).

After the matching process, the position in the space of 32566 (first window) and of 90226 (second window) dominant points was defined. Only a percentage of 3% of these points was deleted after the blunder detection process in the first case, while a 9% was deleted in the second case because of wrong matches caused by the presence of the window glasses. The resulting data was smoothed in order to ease the edges in lines and curves. The results of this work are reported in Figure 4b-c and Figure 5b-c: it can be noticed that the window geometry is complete and only some parts are missing.

4.5 3D modeling

In order to achieve a complete product of the surveyed object, the last phase of the data processing is usually represented by the 3D modeling phase, which allows to obtain a semi-realistic view of the object.

The model can be derived in different ways, such as using the principal geometry of the object [24-27] derived from a photogrammetric plotting or a traditional topographic survey, or from LiDAR data [28-30] or other instruments that allow to carry out 3D point clouds (for instance ToF cameras).

In this work a 3D model of one of the surveyed windows was created using an approach based on the integration of the smoothed edges (breaklines) obtained after the multi-image matching and of the 3D data derived from the ToF camera.

Whatever is the techniques for the 3D modeling phase in order to produce a polygonal model for the best digital representation of the surveyed object or scene some fixings for closing holes, editings of incorrect faces of mesh related to non-manifold parts, are always necessary and time consuming. Those errors are visually unpleasant, but they might cause lighting blemishes due to the incorrect normals and the computer model will also be unsuitable for reverse engineering or physical replicas.

According to the available data of the surveyed object (Figure 6a) some tests have been performed in order to evaluate the potentiality of the surveying techniques employed in this case. A first attempt to generate the 3D model using only the point cloud was performed, which is shown in Figure 6b; then, a 3D model was generated using only the extracted breaklines (Figure 6c). All the models were generated using the 3DReshaper software [31].

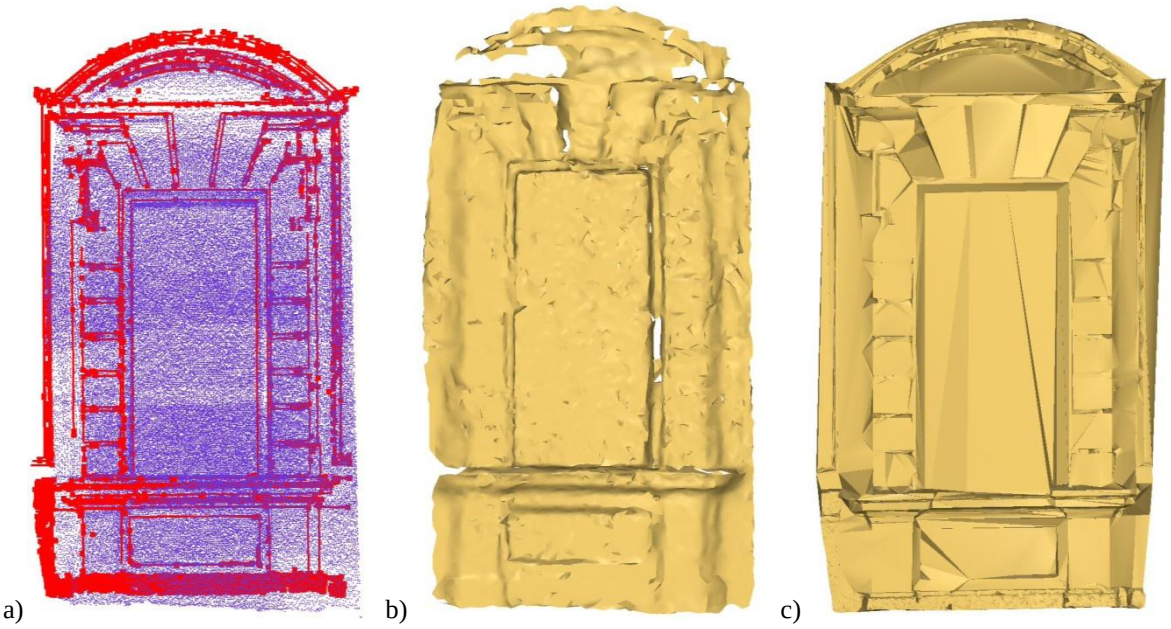

Figure 6. 3D Modeling phase: a) available data (ToF point clouds in blue, edges in red), b) raw 3D model obtained using the ToF point cloud, c) raw 3D model obtained using the extracted breaklines.

As the figures show, the model obtained with the point clouds is more noisy than the second one and due to the triangulation process the details of the real shape of the object are lost (especially the shape of the decoration); on the other hand, using only the breaklines, the window profile is maintained but wrong shapes were obtained after the triangulation process where there is no data.

In order to reduce this errors and to obtain a true 3D model of the window, a final model has been achieved using both data: the ToF point cloud and the breaklines.

The following figures show the final obtained 3D model.

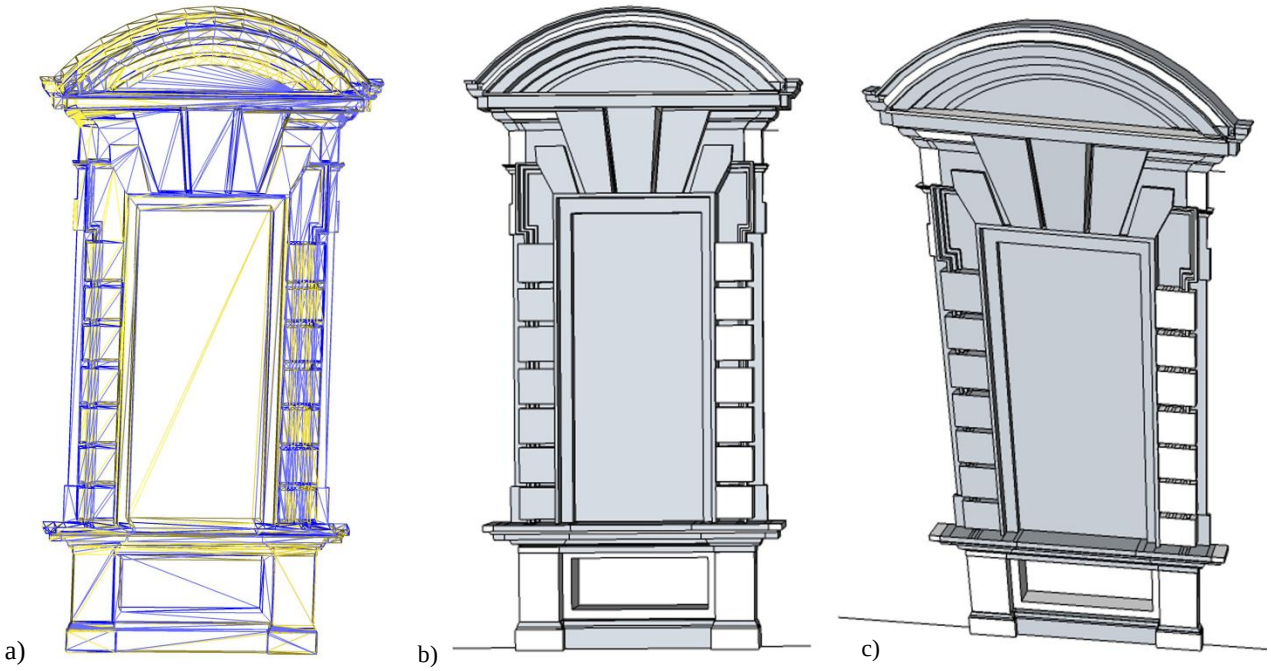

Figure 7. Views of the final 3D model (a) wireframe visualization, b) and c) triangulated surface)

Finally photo-realism [32-36], defined as having no difference between a view rendered from the model and a photograph taken from the same viewpoint, is generally required and obtainable with the texture mapping phase.

In order to achieve a photorealistic view of the surveyed artifact, the texture module of the 3DReshaper software has been employed. Different texturing methods are available; in this case, a photogrammetric approach has been adopted: the faces have been mapped using the external parameters of the oriented images derived from the photogrammetric process. In particular, the origin and orientation of the camera (camera position: X,Y,Z and camera orientation: ω, φ, ,k) and the internal camera geometry (focal length, principal point position and lens distortion), were used in order to achieve correct textures of the window.

Different sets of oriented images were employed in order to achieve more metrically accurate textures.
In Figure 8 some views of the textured window are reported.

Figure 8. Photo-realistic views of one of the surveyed windows

5. CONCLUSIONS AND FUTURE WORKS

The integration between data provided by calibrated Time-of-Flight (ToF) cameras and a multi-image matching technique has been presented in this paper. The ToF data is usually affected by some systematic errors that can be partially corrected by using a suitable calibration procedure, achieving complete 3D point clouds comparable with those of traditional LiDAR acquisitions. The resulting point clouds can be registered and oriented in the photogrammetric coordinate system in order to generate an approximate DSM of the object to be used in a multi-image matching approach. The main drawbacks of the ToF cameras are the low resolution of actual sensors and the maximum unambiguous measurement range (tens of meters), that reduces the extension of the area to be surveyed by a single camera position. On the other hand, range cameras are able to acquire data at video frame rates and they are characterized by low costs and handiness.

The performed tests show that using the ToF DSM, good results can be achieved in the realization of architectural drawings. Using the proposed approach it is possible to drastically reduce both the data acquisition and processing times for 2D and/or 3D rough drawing generation (the drawings reported in this paper were automatically generated using the proposed algorithm). In order to achieve a complete architectural representation, the extracted edges need to be manually edited and eventually integrated.

Future works will try to improve the performances of the integration algorithm and to increase the completeness of the achievable results. Moreover, further investigations will be performed to assess the geometric accuracy of the final drawings, in order to verify the maximum representation scale that can be achieved in order to have a correct metric representation and to limit the editing time for the final drawing production.

Finally, the first results of our research group about 3D modeling of architectural artifacts have been reported, which show the potentiality of data integration (ToF point cloud and object breaklines) to obtain metrically correct 3D models.

REFERENCES

[1] Nex, F., Rinaudo, F., 2009, "New integration approach of Photogrammetric and LIDAR techniques for architectural surveys," Laserscanning 2009, 12-17 (2009).

[2] Nex, F., "Multi-Image Matching and LiDAR data new integration approach," PhD Thesis, Politecnico di Torino, Torino (2010).

[3] Albota, M.A., Heinrichs, R.M., Kocher, D.G., Fouche, D.G., Player, B.E., Obrien, M.E., Aull, G.F., Zayhowski, J.J., Mooney, J., Willard, B.C., Carlson, R.R., "Three-dimensional imaging laser radar with a photon-counting avalanche photodiode array and microchip laser," Applied Optics *41*, 7671-7678 (2002).

[4] Lange, R., "Time-of-Flight range imaging with a custom solid-state image sensor". Proc. SPIE 3823, 180-191(1999).

[5] Anderson, D., Herman, H., Kelly, A., "Experimental Characterization of commercial flash ladar devices," Proceedings of International Conference on Sensing Technologies, Palmerston North, New Zealand (2005).

[6] Kahlmann, T., Remondino F., Ingensand, H., "Calibration for increased accuracy of the range imaging camera Swiss Ranger," International Archives of Photogrammetry, Remote Sensing and Spatial Information Sciences XXXVI, 136-141 (2006).

[7] Lichti, D, "Self-Calibration of a 3D Range Camera 2008," International Archives of Photogrammetry, Remote Sensing and Spatial Information Sciences XXXVII, 927-932 (2008).

[8] Lindner, M., Kolb, A, "Lateral and depth calibration of PMD-distance sensors," Proceedings of ISVC, 524-533 (2006).

[9] Rapp, H., Frank, M., Hamprecht, F.A., Jähne, B., "A theoretical and experimental investigation of the systematic errors and statistical uncertainties of Time-of-Flight-cameras," IJISTA 2008 *5*, 402-413 (2008).

[10] Weyer, C.A., Bae, K., Lim, K., Lichti, D., "Extensive metric performance evaluation of a 3D range camera," International Society of Photogrammetry and Remote Sensing XXXVII, 939-944 (2008).

[11] www.mesa-imaging.ch

[12] Jamtso, S., Lichti, D.D., "Modelling scattering distortion in 3D range camera," International Archives of Photogrammetry, Remote Sensing and Spatial Information Sciences XXXVIII, 299-304 (2010).

[13] Dorrington, A. A., Payne, A. D., Cree, M. J., "An evaluation of time-of-flight range cameras for close range metrology applications," International Archives of Photogrammetry, Remote Sensing and Spatial Information Sciences XXXVIII, 201-206 (2010).

[14] Chiabrando, F., Chiabrando, R., Piatti, D., Rinaudo, F., "Sensors for 3D Imaging: Metric Evaluation and Calibration of a CCD/CMOS Time-of-Flight Camera," Sensors 9, 10080-10096 (2009).

[15] Chiabrando, F., Piatti, D., Rinaudo, F., "SR-4000 ToF camera: further experimental tests and first applications to metric surveys," International Archives of Photogrammetry, Remote Sensing and Spatial Information Sciences XXXVIII, 149-154 (2010).

[16] Zhang, L., "Automatic Digital Surface Model (DSM) generation from linear array images," Thesis Diss. ETH No. 16078, Technische Wissenschaften ETH Zurich, 2005, IGPMitteilung N. 90 (2005).

[17] Habib, A. F., Ghanma, M. S., Tait, M., "Integration of LIDAR and photogrammetry for close range applications," Proc. XXI ISPRS Congress (2004).

[18] Wallis, R., "An approach to the space variant restoration and enhancement of images," Proc. Symposium on Current Mathematical Problems in Image Science, 329- 340 (1976).

[19] Lingua A., Marenchino, D., Nex, F., "Performance analysis of the SIFT operator for automatic feature extraction and matching in photogrammetric applications," SENSORS, 3745-3766, 2009, Vol. 9(5), ISSN: 1424-8220, DOI: 10.3390/s90503745 (2009).

[20] Lingua A., Rinaudo F., "Aerial triangulation data acquisition using a low cost digital photogrammetric system," International Archives of Photogrammetry and Remote Sensing, Vol. XXXIII/B2, 449-454, ISSN: 0256-184 (2000).

[21] Canny, J., "A Computational Approach To Edge Detection," IEEE Trans. Pattern Analysis and Machine Intelligence, 8, 679–714 (1986).

[22] Christmas, W. J., Kittler, J., Petrou, M., "Structural Matching in Computer Vision Using Probabilistic Relaxation," PAMI, Vol. 17, No. 8, 749-764 (1995).

[23] Baltsavias, E., "Multiphoto Geometrically Constrained Matching," Phd. dissertation, ETH Zurich, Switzerland, ISBN 3-906513-01-7 (1991).

[24] Lo Turco, M., Sanna, M., “Digital modelling for architectural reconstruction. the case study of the Chiesa Confraternita della Misericordia in Turin,” International Archives of Photogrammetry, Remote Sensing and Spatial Information Sciences, Vol. XXXVIII-3/W8, 101-106 (2009)

[25] Gibson, S., Hubbold, R. J., Cook, J., Howard,T. L. J., “Interactive reconstruction of virtual environments from video sequences,”Computers & Graphics, 27,293–301 (2003).

[26] Debevec, P., Taylor C. J., Malik, J., “Modelling and rendering architecture from photographs:A hybrid geometry and image-based approach,” Proc. of SIGGRAPH ACM, 11–20 (1996).

[27] Lewis, R., Sequin, C., “Generation of 3D building models from 2D architectural plans,”Computer-Aided Design, 30(10), 765–779 (1998).

[28] Remondino, F., El-Hakim, S.,” Image-based 3D modelling: a review,” Photogrammetric Record, 21(115), 269-291 (2006).

[29] Bonfanti, C., Chiabrando, F., Spanò A.,” High accuracy images and range based acquiring for artistic handworks 3D models,” The international archives of the photogrammetry, remote sensing and spatial information sciences, pp. 6, 2010, vol. XXXVIII/5, 109-114, (2010).

[30] Böhm, J.,” Terrestrial Laser Scanning - A Supplementary Approach for 3D Documentation and Animation”, Photogrammetric Week '05, Fritsch (ed.), Wichmann, 263-271 (2005).

[31] www.3dreshaper.com

[32] Borshukov, G,. New algorithms for modeling and rendering architecture from photographs. Master's thesis, University of California at Berkeley, Computer Science Division, Berkeley, (1997).

[33] Koeva, M., “3D realistic modeling and visualization of buildings in urban areas,” Int sym on Modern technologies, education and professional practice in geodesy and related fields, Sofia, (2004).

[34] Lerma, J. J., Garcia, A., “3D city modelling and visualization of historic centers,” Int workshop on vision techniques applied to the rehabilitation of city centers, 25-27 Oct, Lisbon, Portugal, (2005).

[35] El-Hakim, S. et al., “Effective 3D Modeling of Heritage sites,” 4th Int Conf on 3D Digital Imaging and Modeling, Banff, Canada, October 6-10, 302-309 (2003).

[36] El-Hakim, S. et al., “3D reconstruction of complex architectures from multiple data,” ISPRS Int. Workshop on 3D virtual reconstruction and visualization of complex architectures (3D-Arch 2005), August 22-24, Venice-Mestre, Italy (2005).